Chinese Chemical Letters 35 (2024) 109652

Contents lists available at ScienceDirect

Chinese Chemical Letters

journal homepage: www.elsevier.com/locate/cclet

Adsorption and activation of peroxymonosulfate on BiOCl for carbamazepine degradation: The role of piezoelectric effect

Cunjun Li[a], Wencong Liu[b], Xianlei Chen[a], Liang Li[a], Shenyu Lan[b,c,*], Mingshan Zhu[b,*]

[a] Zhoushan Institute of Calibration and Testing for Quality and Technology Supervision, Zhoushan 316012, China
[b] School of Environment, Jinan University, Guangzhou 511443, China
[c] Department of Environmental Science and Engineering, Xi' an Jiaotong University, Xi'an 710049, China

ARTICLE INFO

Article history:
Received 25 October 2023
Revised 10 January 2024
Accepted 2 February 2024
Available online 10 February 2024

Keywords:
Peroxymonosulfate adsorption
Peroxymonosulfate activation
Electron transfer
BiOCl piezoelectricity
Carbamazepine degradation

ABSTRACT

The adsorption of peroxymonosulfate (PMS) is crucial for PMS activation in the heterogeneous advanced oxidation processes. However, the investigation of PMS adsorption on the piezocatalysts still remains insufficient. In this work, bismuth oxychloride (BiOCl) nanosheets were prepared as the piezocatalysts for PMS activation under ultrasonic vibration to remove carbamazepine (CBZ) in aqueous solutions. Up to 92.5% of CBZ was degraded for 40 min in BiOCl piezo-activated PMS system with the reaction rate constant of 0.0741 min^{-1}, being 1.63 times that of the sum of BiOCl piezocatalysis, BiOCl-activated PMS, and vibration-activated PMS. PMS adsorption on the surface of BiOCl was specifically studied by comparing the microscopic structure change of the fresh and used BiOCl. The results suggested that the piezoelectric field of BiOCl was able to promote the tight adsorption of PMS on the surface, thus facilitating the fast activation of PMS through electrons transfer to produce reactive species ($HO^{\bullet}$, $SO_4^{\bullet-}$, $O_2^{\bullet-}$, $^1O_2$). This work presents an in-depth understanding for the role of piezoelectric effect on the adsorption and activation of PMS.

Carbamazepine (CBZ), an iminostilbene derivative with a tricyclic structure, is a first-choice drug of epilepsy and neuropathic pain [1]. The low biodegradability makes it extensive occurrence in wastewater, and the high toxicity endows it a high threaten on human and ecosystem even at low concentrations [2,3]. Therefore, it is an urgent to develop an effective method to remove CBZ from aqueous solution. Advanced oxidation processes (AOPs) are the primary way to remove emerging organic contaminates due to the production of reactive oxygen species such as sulfate radical ($SO_4^{\bullet-}$), hydroxyl radical ($HO^{\bullet}$), superoxide radical ($O_2^{\bullet-}$) and singlet oxygen ($^1O_2$) [4–6]. Peroxymonosulfate (PMS) has been widely applied in AOPs after activation through energy input or electron transfer, such as heat, alkaline, ultraviolet radiation, transition metals, heterogeneous catalysis [7–9]. Among them, the heterogeneous catalysis is regarded a promising way owing to its wide pH tolerance, high catalytic stability, and non-metal ions leaching.

Piezoelectricity, the ability of the heterogeneous material to develop electrical behavior in response to the applied mechanical stress [10], provides an attractive platform for PMS activation. When a piezoelectric material is deformed under the mechanical stress, the displaced atoms would gain a nonzero dipole moment to induce the production of electric polarization to separate the free charges [11]. These charges would directly trigger redox reactions for water splitting and environmental remediation, *i.e.*, piezocatalysis [12,13], as well as have a great potential to facilitate the activation of reactants, *e.g.*, destroying the O–O bond of PMS to make it activation [14]. For example, the piezo-generated charges of $BaTiO_3$ under the external stress have been reported to break O–O bond within PMS molecule to induce its activation for the benzothiazole removal [15]. The oxygen vacancies and mesoporous superstructures of ZnO can promote the electron and mass transfer, and decrease the reaction barriers of PMS activation [16].

For the PMS activation process by the heterogeneous piezoelectricity, PMS molecules are firstly bound to the surface of catalyst by chemisorption, and then the piezo-induced electrons transfer from catalyst to PMS molecules for the direct dissociation of peroxide O–O bond. From this point of view, PMS activation mainly occurred on the surface of catalyst, hence, the adsorption of PMS on the surface of catalyst may be the key step for its activation. However, the reported studies rarely pay attention to PMS adsorption during the piezo-activation process, and the mechanisms of PMS adsorption/activation by piezoelectricity are still not clear. Therefore, it is

* Corresponding authors.
E-mail addresses: lanshenyu@xjtu.edu.cn (S. Lan), zhumingshan@jnu.edu.cn (M. Zhu).

https://doi.org/10.1016/j.cclet.2024.109652
1001-8417/

necessary to comprehensively investigate the adsorption/activation process of PMS, and further establish the relationships between the piezoelectric property and the adsorption/activation of PMS.

Considering that bismuth oxychloride (BiOCl) is an interesting piezoelectric material [17–19] with the layered structure consisting of $[Bi_2O_2]^{2+}$ slabs interleaved by double Cl^- slabs [20,21]. The ultrathin structure with internal static electric field along the *c* axis allows driving redox reactions through piezoelectric process. In this work, we would prepare BiOCl nanosheets through a simple hydrothermal method, and study its piezo-activity for PMS activation through employing CBZ as the model organic contaminant. All materials, preparation of catalysts, experimental procedures, and analysis methods are shown in Text S1 (Supporting information). The piezo-property of BiOCl, the piezo-activation performance and mechanism for PMS, as well as the relationship of adsorption and activation of PMS would be studied in detail. Overall, this study provides a new understanding for PMS activation by piezoelectricity in the oxidation of organic pollutants.

The well-crystallized and layered BiOCl nanosheets with a square-like morphology (Figs. S1 and S2 in Supporting information) are prepared as the piezocatalysts for PMS activation. The piezoelectric behavior of BiOCl is firstly demonstrated through the piezo-response force microscopy. The three-dimensional topography of BiOCl presents a non-homogeneous layer scanned in a $5 \times 5\ \mu m^2$ area (Fig. 1A). The phase and amplitude hysteresis (Fig. 1B) are obtained by applying -40 V to $+40$ V electric field across the sample. It is noted that the sample gives a saturated phase loop with 180 °C domains, implying the existence of well-defined polarizations along the field direction. The amplitude loop clearly shows a typical butterfly shape, which is ascribed to the piezoelectric properties of BiOCl.

The piezo-current density of BiOCl nanosheets are determined within the various voltages (Fig. 1C). Obviously, the improvement of current density under ultrasonic stress is ascribed to the mediating piezoelectric potential, which greatly promote the separation and migration of charge carriers. The reduction of Au^{3+} is used as a probe reaction to verify the piezoelectric redox reaction, as the preferential deposition of Au metal reflects the migration of electrons. From the UV–vis diffuse reflectance spectra (Fig. 1D), the characteristic surface plasma resonance peak of Au nanoparticle appears at about 560 nm after adding BiOCl to the solution containing Au^{3+} and ultrasonic vibration. It further proves that the piezoelectric property of BiOCl is able to drive the occurrence of redox reaction.

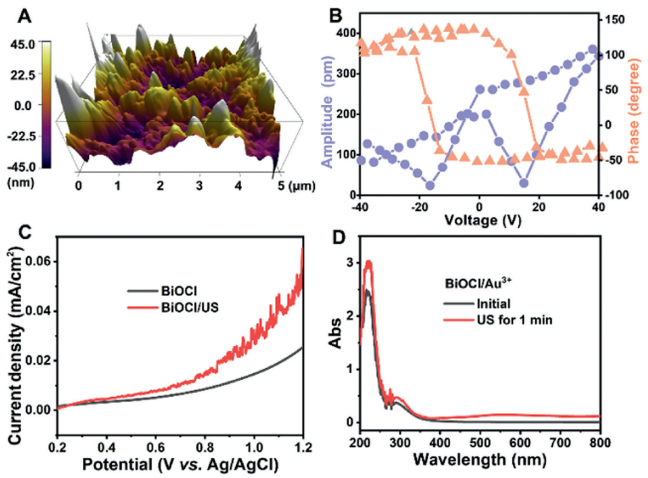

Fig. 1. (A) AFM topography, (B) PFM phase hysteresis loops and amplitude hysteresis, (C) Piezo-current density *versus* potential curve, (D) UV–vis spectra of BiOCl and Au-BiOCl, US refers to ultrasonic vibration.

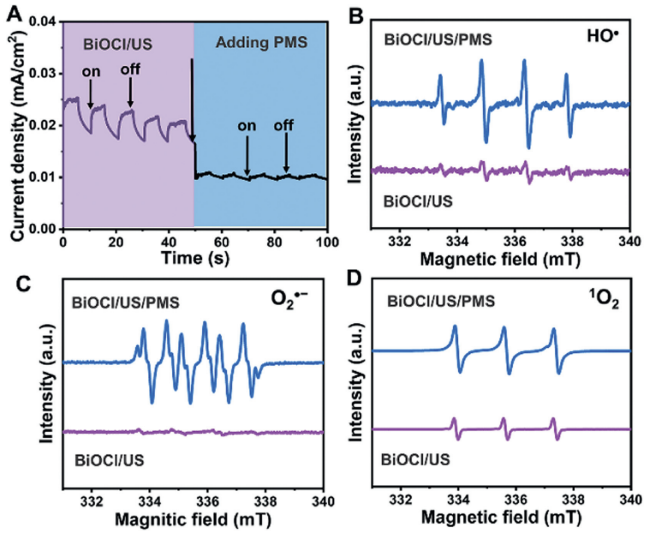

Fig. 2. (A) Transient piezo-current profiles without and with PMS. Electron paramagnetic resonance spectra of (B) $HO^•$, (C) $O_2^{•-}$ and (D) $^1O_2$ in piezocatalytic system and piezo-activated PMS system.

Fig. 2A shows the piezoelectric current variation of BiOCl in the presence or absence of PMS. The piezo-current increases when the ultrasonic cleaner is turned on, whereas falls back when the ultrasonic cleaner is turned off. It suggests the generation and transportation of piezoelectric electrons under the external press. What is more, when PMS is added in the BiOCl piezoelectric system, the current density is instantly decreased, indicating that the presence of PMS consumes the generated electrons in the piezoelectric process. After PMS is consumed, more reactive oxygen specials would generate, which is verified *via* electron paramagnetic resonance (EPR) spectra of BiOCl with or without PMS under ultrasonic vibration (Figs. 2B–D). The characteristic peaks of $HO^•$ with intensity of 1:2:2:1 can be found, while the peak intensity of $SO_4^{•-}$ is rather weak due to the fast conversion of $SO_4^{•-}$ into $HO^•$ radicals [22,23]. At the same time, the corresponding EPR spectral of $O_2^{•-}$ and a three-signal peak of $^1O_2$ are also observed [24]. Obviously, the intensities of all reactive oxygen species in BiOCl piezo-activated PMS system are higher than that of individual BiOCl piezocatalysis. The above results indicate that the piezoelectric effect of BiOCl can active PMS through electron transfer for promoting the generation of reactive oxygen species.

The ability of BiOCl piezo-activated PMS is further evaluated by CBZ degradation in the different reaction systems. As shown in Fig. 3A, only 2.7%, 3.6%, and 4.6% of CBZ is respectively removed within 40 min during PMS self-oxidation, BiOCl adsorption, and ultrasonic vibration, so the contribution of PMS alone, BiOCl alone, or US alone could be neglected for CBZ degradation. When BiOCl and PMS are used together, about 8.1% of CBZ is removed, suggesting BiOCl has a limited ability for PMS activation. The degradation efficiency of CBZ is about 15.2% in the presence of ultrasonic vibration and PMS, meaning that the vibration also has a weak ability to active PMS. Moreover, when both BiOCl and US are present in the reaction system, the removal efficiency of CBZ reaches 77.1%. It reveals that the ultrasonic can drive the deformation of BiOCl to produce piezo-effect to participated in redox reaction for CBZ degradation. Significantly, when the piezoelectric process of BiOCl is joined in the PMS oxidation, the removal efficiency of CBZ is improved up to 92.5%, which is 15.4% higher than that in BiOCl piezocatalytic system, 77.3% higher than that in US-activated PMS system, and 84.4% higher than that in BiOCl-activated PMS system. The results convincingly reveal that the combination of US, BiOCl and PMS can

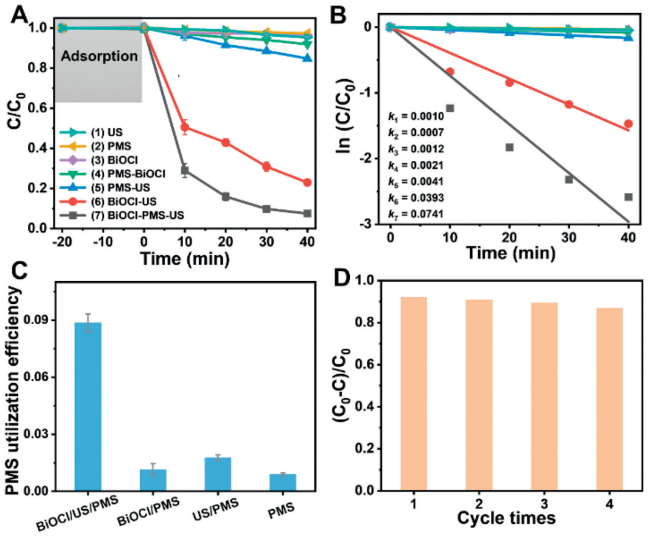

Fig. 3. (A) Degradation efficiencies and (B) kinetic fittings of CBZ as a function of reaction time in different systems. (C) PMS utilization efficiency in different systems. (D) Recycling tests of CBZ degradation in BiOCl piezo-activated PMS process. Conditions: [CBZ] = 5 mg/L, [BiOCl] = 0.5 g/L, [PMS] = 1 g/L, US refers to ultrasonic vibration with 40 kHz and 100 W.

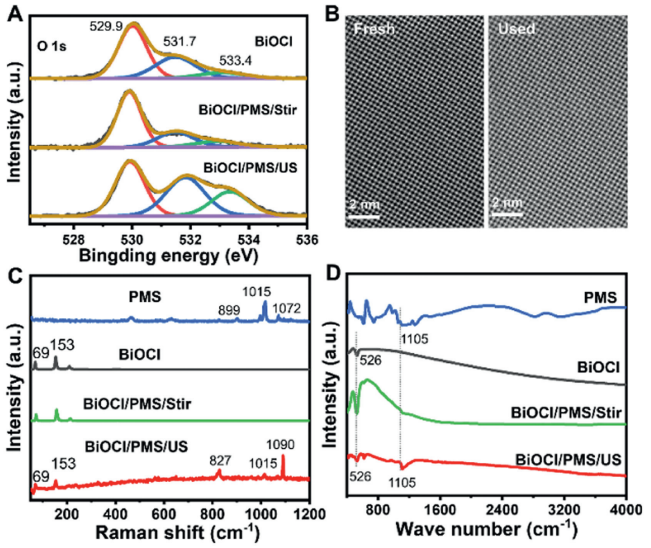

Fig. 4. (A) XPS spectra of O 1s, (B) STEM of fresh and used BiOCl, (C) Raman spectra of BiOCl or PMS, (D) FTIR spectra of BiOCl or PMS.

efficiently remove CBZ in aqueous solution. Fig. 3B shows that the *pseudo* first-order rate constants in the processes of BiOCl/PMS, US/PMS, and BiOCl/US are 0.0021, 0.0041 and 0.0393 min^{-1}, respectively. The constant increases to 0.0741 when combining BiOCl, PMS and ultrasonic together, which is 1.63 times that of the sum of the former three processes, exhibiting an obvious synergistic effect. This result strongly proves that BiOCl piezoelectric process is able to effectively activate PMS for enhancing CBZ degradation.

In order to further provide insight on the role of piezo-effect on PMS activation, the PMS utilization efficiency is calculated in Fig. 3C by correlating the PMS decomposition and CBZ degradation of all tested systems. Obviously, the utilization efficiency of PMS in the BiOCl/PMS/US system is up to 0.0852, being much higher than other systems, so it has the significant advantage of degrading CBZ. In order to study the stability and recyclability of heterogeneous catalysts for practical application, the performance of BiOCl piezo-activated PMS is further evaluated in the four consecutive cycling experiments for CBZ degradation. As shown in Fig. 3D, the removal performance of CBZ almost has no remarkable decreases even after four runs, indicating that the reused catalyst has the long-term potential and high reusability. The effect of catalyst dosage, PMS concentration and ultrasonic power are also investigated in Figs. S3-S5 (Supporting information). Obviously, the increasing catalyst dosages provide increasing active sites for improving CBZ removal. The increasing PMS concentration produce increasing reactive species with at a certain range, while excess PMS would exhaust the reactive species through self-quenching reaction. And a higher ultrasonic power can lead to a larger deformation of BiOCl and a stronger piezoelectric field, thus more electrons would activate PMS to generate reactive oxygen species for CBZ removal.

X-ray photoelectron spectroscopy (XPS) analysis of the fresh and used BiOCl are conducted to better understand the reaction process for PMS activation. The two peaks at 165.0 and 159.5 eV are assigned to the binding energies of Bi $4f_{5/2}$ and Bi $4f_{7/2}$ of Bi^{3+} (Fig. S6a in Supporting information). The typical peaks at 198.1 eV and 199.7 eV (Fig. S6b in Supporting information) are attributed to Cl $2p_{3/2}$ and Cl $2p_{1/2}$, respectively. There are no changes of Bi and Cl element before and after the reaction. For O 1s spectra, the lattice oxygen (Bi–O) at 529.9 eV also has no change from Fig. 4A. However, the peaks of oxygen-containing group located at 531.7 eV and 533.4 eV significantly increase after PMS piezo-activation [25]. Then we employ EPR spectra and STEM images to clarify these changes. Results show that there is no characteristic EPR signal of vacancy oxygen and no defective structures, such as lattice distortion and missing atoms, in the STEM images of Fig. 4B, which exclude the formation of oxygen vacancies. Therefore, the increasing peaks of oxygen-containing group may be ascribed to that the catalytic sites are occupied by surface adsorbed oxygen-containing groups, *e.g.*, OH^- or HSO_5^-.

In order to confirm the above possibility, the structural properties of the fresh and used BiOCl are further compared by Raman spectrum and FTIR spectrum (Figs. 4C and D). In the Raman spectra, the bands of PMS at about 899, 1015 and 1072 cm^{-1} are identified as the S–O stretching vibration of HSO_5^-. All the peaks of PMS are not be found in BiOCl/PMS/Stir system, but remain in BiOCl/PMS/US system. Compared with pure PMS, the characteristic vibration peaks have shifts from 899 to 827 cm^{-1} and from 1072 cm^{-1} to 1090 cm^{-1} in BiOCl piezo-activated system. It is because the peroxide bond firmly interacts with BiOCl to change the stretching vibration amplitude [26]. These results suggest the piezoelectric process can boost PMS adsorption and finally bond to surface sites for activation. In the FTIR spectra, the band at 1105 cm^{-1} in BiOCl piezo-activated PMS is identified as the S–O stretching vibration of HSO_5^- [27], which is comparable with the pure PMS. The above results vividly demonstrate the contribution of piezoelectricity that the S–O–(OH) structure of HSO_5^- are much easier to bonded to the catalyst surfaces in the presence of piezoelectricity, which is benefit for PMS activation through electron transfer from catalyst to PMS molecule.

After being adsorbed on the surface of catalyst, the piezo-induced electrons would cleave the O–O bond of PMS through electron transfer to generate reactive oxygen species for attacking CBZ molecule. The radical scavenging tests are conducted to determine the contribution of different reactive oxygen species for CBZ degradation in BiOCl/US/PMS system (Fig. S7 in Supporting information). About 63.4%, 75.8% and 79.7% of CBZ are removed from aqueous solution containing methanol, EDTA-2Na and TBA, indicating that $SO_4^{\bullet-}$, h^+ and $HO^\bullet$ have insignificant roles for the degradation of CBZ [28,29]. In presence of FFA, $K_2Cr_2O_7$ and p-BQ, the scavengers of $^1O_2$, e^- and $O_2^{\bullet-}$ [30,31], only 9.7%, 15.9% and 20.2% of CBZ are respectively degraded. The strong inhibitory effects im-

ply the main roles of $^1O_2$, e^- and $O_2^{\bullet-}$ for CBZ degradation. According to DFT computation and LC-MS analysis, the Fukui index and the possible degradation pathways of CBZ were proposed in Figs. S8 and S9 (Supporting information). C11 and C13 with high values are active sites for attacking, resulting in the generation of bond cleavage (pathway I), epoxide (pathway II) [32], and hydroxyl substitution (pathway III) [33]. C21 and C1 are also relative active to form pathway IV through hydroxyl substitution. After the cleavage of saturated rings, ring contraction/shrinkage, and deamination reaction, the generated intermediates are transformed into small molecules, and even mineralized into NO_3^-, CO_2 and H_2O.

Based on the above information, the overall mechanisms of the BiOCl piezo-activated PMS for CBZ oxidation are deduced in Scheme S1 (Supporting information) and Eqs. 1–9. Firstly, the electrons and holes are produced in the BiOCl nanosheets under the applying force [34]. Then, the generated electrons activate PMS to generate $SO_4^{\bullet-}$ and $HO^\bullet$ radicals. At the same time, the electrons and holes respectively combine with the dissolved oxygen and water molecules to generate $O_2^{\bullet-}$ and $HO^\bullet$ [35]. In addition, $HO^\bullet$ can react with $O_2^{\bullet-}$ to generate $^1O_2$, dissolved oxygen can be converted into $^1O_2$, and PMS anions also can react with itself to produce $^1O_2$ [36].

$$BiOCl + \text{mechanical force} \rightarrow BiOCl + e^- + h^+ \quad (1)$$

$$HSO_5^- + e^- \rightarrow SO_4^{\bullet-} + OH^- \quad (2)$$

$$HSO_5^- + e^- \rightarrow SO_4^{2-} + HO^\bullet \quad (3)$$

$$SO_4^{\bullet-} + H_2O \rightarrow SO_4^{2-} + HO^\bullet + H^+ \quad (4)$$

$$O_2 + e^- \rightarrow O_2^{\bullet-} \quad (5)$$

$$H_2O + h^+ \rightarrow H^+ + HO^\bullet \quad (6)$$

$$O_2^{\bullet-} + HO^\bullet \rightarrow OH^- + {}^1O_2 \quad (7)$$

$$O_2 + h^+ \rightarrow {}^1O_2 \quad (8)$$

$$HSO_5^- + SO_5^{2-} \rightarrow SO_4^{2-} + HSO_4^- + {}^1O_2 \quad (9)$$

In summary, we have demonstrated an effective protocol to improve the degradation of organic pollutants by association of PMS oxidation with the piezoelectric effect. Through a comprehensive study, it is found that the piezoelectric process of BiOCl can effectively activate PMS for CBZ removal, which was attributed to the tight adsorption and the fast activation of PMS induced by piezoelectric effect. This work is dedicated to the in-depth understanding into PMS adsorption/activation over BiOCl samples, which is of critical importance to reveal the intrinsic role of piezoelectric effect in the adsorption/activation of PMS for pollutant decomposition.

Declaration of competing interest

The authors declare that they have no known competing financial interests or personal relationships that could have appeared to influence the work reported in this paper.

Acknowledgments

The present study was financially supported by the National Natural Science Foundation of China (No. 22006052), and the Science and Technology Program of Guangzhou, China (No. 202201020545).

Supplementary materials

Supplementary material associated with this article can be found, in the online version, at doi:10.1016/j.cclet.2024.109652.

References

[1] N. Vieno, H. Härkki, T. Tuhkanen, et al., Environ. Sci. Technol. 41 (2007) 5077–5084.
[2] F. Pomati, S. Castiglioni, E. Zuccato, et al., Environ. Sci. Technol. 40 (2006) 2442–2447.
[3] D. Guo, S. You, F. Li, et al., Chin. Chem. Lett. 33 (2022) 1–10.
[4] D.B. Miklos, C. Remy, M. Jekel, et al., Water Res. 139 (2018) 118–131.
[5] C. Zhai, Y. Chen, X. Huang, et al., Env. Funct. Mater. 1 (2022) 219–229.
[6] C. Yu, J. He, S. Lan, et al., Environ. Sci. Ecotechnol. 10 (2022) 100165.
[7] O.S. Furman, A.L. Teel, R.J. Watts, Environ. Sci. Technol. 44 (2010) 6423–6428.
[8] C. Pu, Gang Lu, H. Qi, et al., J. Struct. Chem. 42 (2023) 100093.
[9] Z. Li, S. Lan, M. Zhu, Environ. Sci. Ecotechnol. 18 (2024) 100329.
[10] Y. Liu, Y. Zhang, Q. Yang, et al., Nano Energy 14 (2015) 257–275.
[11] Z.L. Wang, Adv. Mater. 24 (2012) 280–285.
[12] M. Wang, B. Wang, F. Huang, et al., Angew. Chem. Int. Ed. 58 (2019) 7526–7536.
[13] Z. Liang, C.F. Yan, S. Rtimi, et al., Appl. Catal. B: Environ. 241 (2019) 256–269.
[14] Y. Chen, S. Lan, M. Zhu, Chin. Chem. Lett. 32 (2021) 2052–2056.
[15] S. Lan, Y. Chen, L. Zeng, et al., J. Hazard. Mater. 393 (2020) 122448.
[16] M. Zhang, H. Tao, C. Zhai, et al., Appl. Catal. B: Environ. 326 (2023) 122399.
[17] D. Shao, L. Zhang, S. Sun, et al., ChemSusChem 11 (2018) 527–531.
[18] Y. Zhou, H. Dong, Z. Xu, et al., Appl. Catal. B: Environ. 343 (2023) 123504.
[19] Y. Long, H. Xu, J. He, et al., Surf. Interfaces 31 (2022) 102056.
[20] J. Jiang, K. Zhao, X. Xiao, et al., J. Am. Chem. Soc. 134 (2012) 4473–4476.
[21] M. Li, S. Yu, H. Huang, et al., Angew. Chem. Int. Ed. 58 (2019) 9517–9521.
[22] J. Wang, S. Wang, Chem. Eng. J. 401 (2020) 126158.
[23] Y. Guan, J. Ma, X. Li, et al., Environ. Sci. Technol. 45 (2011) 9308–9314.
[24] Q. Liu, H. Li, H. Zhang, et al., Chin. Chem. Lett. 33 (2022) 4756–4760.
[25] C. Li, S. Yi, Y. Liu, et al., Chem. Eng. J. 417 (2021) 129231.
[26] Y. Ren, L. Lin, J. Ma, et al., Appl. Catal. B: Environ. 165 (2015) 572–578.
[27] T. Zhang, H. Zhu, J.-P. Croue, Environ. Sci. Technol. 47 (2013) 2784–2791.
[28] R. Yin, Y. Chen, S. He, et al., J. Hazard. Mater. 388 (2020) 121996.
[29] Z. Xin, X. Zhao, H. Ji, et al., Chin. Chem. Lett. 32 (2021) 2151–2154.
[30] H. Jiang, Q. Wang, P. Chen, et al., J. Clean. Prod. 339 (2022) 130771.
[31] L. Jin, S. You, N. Ren, et al., Environ. Sci. Technol. 56 (2022) 11750–11759.
[32] Q. Huo, X. Qi, J. Li, et al., Appl. Catal. B: Environ. 255 (2019) 117751.
[33] Y. Guo, Y. Ao, P. Wang, et al., Appl. Catal. B: Environ. 254 (2019) 479–490.
[34] M. Zhang, W. Guo, Y. Chen, et al., Chin. Chem. Lett. 34 (2023) 108229.
[35] W. Zheng, Y. Liu, F. Liu, et al., Water Res. 223 (2022) 118994.
[36] Y. Jiang, Z. Xiong, J. Huang, et al., Chin. Chem. Lett. 33 (2022) 415–423.